

Optical fiber refractometer using narrowband cladding-mode resonance shifts

Chun-Fan Chan, Chengkun Chen, Amir Jafari, Albane Laronche, Douglas J. Thomson, and Jacques Albert

Short-period fiber Bragg gratings with weakly tilted grating planes generate multiple strong resonances in transmission. Our experimental results show that the wavelength separation between selected resonances allows the measurement of the refractive index of the medium surrounding the fiber for values between 1.25 and 1.44 with an accuracy approaching 1×10^{-4} . The sensor element is 10 mm long and made from standard single-mode telecommunication grade optical fiber by ultraviolet light irradiation through a phase mask. © 2007 Optical Society of America

OCIS codes: 060.2370, 120.5710, 230.1480.

1. Introduction

Refractometry is used in many important areas including industrial process monitoring, quality control in the food industry, and biomedical applications. Most refractometers in use today are derived from the Abbe refractometer.¹ This instrument measures refractive indices of liquids and solids by determining changes in the angle of total internal reflection for a high index prism on which the material with the unknown refractive index is placed in contact. While these instruments can be very accurate (down to 10^{-5} precision on refractive index for advanced refractometers), they cannot be used in all situations because of their size, power requirements, or the manner in which the liquid or solid substance must be put in contact with the prism. Therefore there is a need for miniature, minimally invasive refractometers that could be used by immersion in liquids or gases of interest (often constrained in small areas) and interrogated remotely. Fiber-optic versions have been developed for this purpose, in which the sensor is a fiber grating embedded in the core of the fiber.^{2–11} In fiber form, such a refractometer allows “lab-on-a-fiber” ap-

plications where chemical species in gas or liquid phase are detected through changes in the refractive index of a functional sensing layer deposited on the fiber.⁴

To measure refractive index changes by monitoring the resonant wavelengths of fiber gratings, the guided light must be brought in contact with the outer boundary of the fiber cladding so that the evanescent field of the modes penetrates the surrounding medium where the index is to be measured. There are three conventional ways to do this: (1) etch down the fiber cladding to a value small enough so that the core-guided light still has nonzero amplitude at the cladding-outside medium boundary;^{5,6} (2) use a long period grating (LPG) to couple core-guided light to forward-propagating cladding modes^{2–4,7,8}; (3) use a tilted fiber Bragg grating (TFBG) to couple core-guided light to backpropagating cladding modes.^{9–11}

Of these approaches, LPGs have attracted the most attention by far, because they are relatively easy to fabricate, do not generally involve physical modifications of the fiber, and provide well-isolated broad resonances that can be made extremely sensitive to various measurands by proper choice of the cladding mode involved. There are problems however with all the techniques mentioned above: in all cases it is difficult to achieve high sensitivity over a large range of refractive index values with a single sensor; etched fibers have significantly reduced mechanical strength; finally LPG sensors suffer from large cross sensitivity to many kinds of perturbation (such as temperature and bending), not just refractive index change. In the case of TFBGs, the first implementation of a refractometer was based on measuring the normalized envelope of the cladding-mode resonance

C. Chan and D. J. Thomson are with the Department of Electrical and Computer Engineering, University of Manitoba, 75A Chancellor's Circle, Winnipeg, Manitoba R3T 5V6, Canada. C. Chen, A. Jafari, A. Laronche, and J. Albert (jacques_albert@carleton.ca) are with the Department of Electronics, Carleton University, 1125 Colonel By Drive, Ottawa, Ontario K1S 5B6, Canada.

Received 30 August 2006; accepted 16 October 2006; posted 19 October 2006 (Doc. ID 74568); published 12 February 2007.

0003-6935/07/071142-08\$15.00/0

© 2007 Optical Society of America

spectrum in transmission, and it was then shown that this parameter was relatively insensitive to temperature, thereby eliminating one of the problems with LPGs.⁹ Another reason for using the envelope of the resonance spectrum is that this parameter changes monotonically and smoothly for refractive index values between 1.32 and 1.42, with little change in sensitivity per unit refractive index change. We propose instead to use individual TFBG resonances as a measuring parameter and to use the core mode (Bragg) resonance as a wavelength and power level reference. Thus, instead of using an absolute wavelength measurement for the position of a cladding-mode resonance we use a relative measurement, the wavelength separation of the resonance with the Bragg wavelength.¹¹ By definition, the wavelength of the Bragg resonance is totally independent of the refractive index of the outside medium.¹² This eliminates the requirement of absolute wavelength accuracy on the sensor interrogator system since only wavelength differences within a measurement are needed. Furthermore, in spite of the fact that TFBGs couple to a multitude of cladding modes simultaneously, it will be demonstrated that there are wavelength windows where individual resonances can be followed without ambiguity for high-resolution measurements. Although not demonstrated here, the power level of the core-mode resonance can also be used as a reference value if the interrogation system requires knowledge of the absolute power level in the fiber. To quantify the accuracy and ultimate sensitivity of our method, experiments and corroborative simulations are presented for measurements of the refractive index of sugar solutions and calibrated liquids.

2. Theory of the TFBG Sensing Mechanism

TFBGs are short-period gratings in which the grating planes are slanted or blazed with respect to the fiber axis. In a single-mode fiber, the tilt of the grating planes enhances the coupling of the light from the forward-propagating core mode to backward-propagating cladding modes and reduces the coupling to the backward core mode.^{9,12} Therefore, in the transmission spectrum both a core-mode resonance and several cladding-mode resonances appear. In the work presented here, small tilt angles are used so that there is a residual core-mode reflection notch in the transmission spectrum (Fig. 1). The cladding-mode resonances appear at discrete wavelengths shorter than the core-mode Bragg resonance and have the same linewidth as the Bragg resonance, typically 100 pm for a 1 cm long grating near 1550 nm. The cladding modes are guided by the cladding boundary, and as a result, their effective index depends on the refractive index of the outer medium. The sensitivity of the cladding-mode effective index to changes in the external index increases with mode order since the penetration depth of the evanescent field increases for higher-order modes (Fig. 1). By monitoring the shifts of the cladding modes relative to the Bragg resonance, an accurate measure of the surrounding refractive index (SRI) can be obtained.

The range of SRI that can be measured with a single resonance depends on the accuracy with which we can measure the position of the resonance (this is related to the width of the resonance) and on the distance between neighboring resonances: since the resonance position is not known *a priori*, if the resonance has moved by more than the interresonance spacing, it will be confused with a much smaller displacement of its neighboring resonance. For conventional telecommunication grade optical fibers, the interresonance spacing increases from 400 pm near the Bragg resonance to over 1000 pm for resonances located 30 nm away (on the blue side) from the Bragg resonance.

In practice, the Bragg wavelength λ_B is related to the core-mode effective index at that wavelength [$n_{\text{eff}}(\lambda_B)$] and to the period of the grating (Λ) by¹²

$$\lambda_B = 2n_{\text{eff}}\Lambda, \quad (1)$$

where Λ is the projection of the actual grating period Λ_g along the fiber axis due to the tilt angle θ :

$$\Lambda = \Lambda_g / \cos \theta. \quad (2)$$

Similarly, cladding-mode resonances can be found through⁹

$$\lambda_C(i) = (n_{\text{eff}}(i) + n_C(i))\Lambda, \quad (3)$$

where $n_{\text{eff}}(i)$ is the effective index of the core mode at the wavelength of the i th cladding-mode resonance, and $n_C(i)$ is the cladding-mode effective index *at the same wavelength*. Now if we consider the wavelength separation between the Bragg resonance and one of the cladding-mode resonances, we can estimate the sensitivity of this parameter to various perturbations. In the case of changes of the external medium refractive index n_{ext} , the differential shift (change in wavelength separation) is due entirely to the dispersion of the cladding-mode effective index, multiplied by the grating period:

$$\Delta(\lambda_B - \lambda_C(i)) / \Delta n_{\text{ext}} = -\Lambda \partial n_C(i) / \partial n_{\text{ext}}. \quad (4)$$

We can also obtain the temperature dependence of the relative wavelength shift of the Bragg resonance and cladding-mode resonances by differentiating Eqs. (1) and (3), respectively. We then get

$$\Delta \lambda_B / \Delta T = 2(\Lambda \partial n_{\text{eff}} / \partial T + n_{\text{eff}} \partial \Lambda / \partial T), \quad (5)$$

$$\Delta \lambda_C(i) / \Delta T = \Lambda(\partial n_{\text{eff}}(i) / \partial T + \partial n_C(i) / \partial T) + (n_{\text{eff}}(i) + n_C(i)) \partial \Lambda / \partial T. \quad (6)$$

Since most fibers (and certainly the fibers used in this study) have a very small composition difference between the core and the cladding glass ($\sim 3\%$ substitution of Si atoms by Ge atoms in our case), we can expect the thermo-optic coefficients ($\partial n / \partial T$) for the

refractive index of the core and cladding glasses to be similar and close to the value for pure silica, approximately $11 \times 10^{-6}/^{\circ}\text{C}$.¹³ Under these conditions, and for typical grating periods near 500 nm (to get Bragg and cladding-mode resonances in the 1500–1600 nm wavelength region) the first terms on the right-hand side of Eqs. (5) and (6) will add up to a worst-case value near

$$\Lambda(2\partial n_{\text{eff}}/\partial T - \partial n_{\text{eff}}(i)/\partial T - \partial n_c(i)/\partial T)/^{\circ}\text{C} < \Lambda \times 10^{-5} \\ = 5 \text{ pm}/^{\circ}\text{C}. \quad (7)$$

Furthermore we can use the coefficient of thermal expansion of silica ($0.55 \times 10^{-6}/^{\circ}\text{C}$)¹³ in lieu of $(1/\Lambda) \partial \Lambda/\partial T$ to get the relative shift in the resonances due to thermal expansion [from the second terms on the right-hand side of Eqs. (5) and (6)]:

$$\Lambda * 0.55 \times 10^{-6} (2n_{\text{eff}} - n_{\text{eff}}(i) - n_c(i))/^{\circ}\text{C} < 0.12 \text{ pm}/^{\circ}\text{C}, \quad (8)$$

where we have used the fact that both n_{eff} and $n_{\text{eff}}(i)$ lie between 1.446 and 1.448 over the wavelength range of interest (1500–1600 nm) and that $n_c(i)$ can be as low as n_{ext} . For the worst-case estimate given above, the following values were taken: $n_{\text{eff}} = 1.446$, $n_{\text{eff}}(i) = 1.448$, and $n_c(i) = 1.0$ [$n_{\text{eff}}(i)$ is always larger than n_{eff} because of dispersion]. As a result, if we use the distance between the Bragg resonance and one of the cladding-mode resonances to measure the SRI, our measurement of $\Delta(\lambda_B - \lambda_c(i))$ will have a cross sensitivity to temperature of the order of a few picometers per degrees centigrade. Experimentally, we have obtained a cross sensitivity of 0.5 pm/ $^{\circ}\text{C}$ or less for most resonances of a 6 $^{\circ}$ TFBG measured between -10° and $+70^{\circ}\text{C}$ (Ref. 14) (Laffont and Ferdinand⁹ observed as much as 3 pm/ $^{\circ}\text{C}$ of differential shift for a high-order resonance in their TFBGs with 16 $^{\circ}$ of tilt, the difference being likely due to the different type of fiber used and/or the large tilt angle). Another parameter that could adversely affect the resolution of the SRI measurements is strain on the fiber, since Chen and Albert previously demonstrated differential shifts greater than 150 pm for strains of the order of 0.4%.¹⁴ However in refractometry applications, it is conceivable that the fiber in which the grating is written can be packaged in such a way that minimal strains occur during the measurements. One such implementation will be presented below.

To summarize this section, we have demonstrated that the wavelength spacing between a cladding-mode resonance and the Bragg reflection has a sensitivity to external refractive index of the order of $5 \times 10^5 \text{ pm} \times (\partial n_c(i)/\partial n_{\text{ext}})$ with a cross sensitivity to temperature below 0.5 pm/ $^{\circ}\text{C}$, provided no significant strain is imposed on the grating section. It will be demonstrated below that the magnitude of the SRI sensitivity for conventional fibers can be as large as 10,000 pm per unit of refractive index change (u.r.i.), therefore providing a cross sensitivity to temperature

of the order of 0.05% for temperature fluctuations of 10 $^{\circ}\text{C}$ (typical of controlled environments, such as laboratories and *in vivo* applications).

3. Experimental Methods

The basic idea in this experiment is to measure the transmission spectrum of a TFBG immersed in different media with known refractive indices and to record the positions of suitable resonances as a function of SRI. One centimeter long tilted gratings are inscribed in hydrogen-loaded Corning SMF-28 fibers using a pulsed KrF excimer laser and the phase mask technique.^{15,16} The grating period for most samples was 536 nm. The internal tilt angle of the gratings used for the SRI measurement was 4 $^{\circ}$. The transmission spectra were recorded using a JDS Uniphase swept wavelength system with a wavelength resolution of 3 pm using the average of four measurements taken with orthogonal polarization states. All the readings are done at room temperature, which was kept near 23 $^{\circ}\text{C}$. To keep the strain on the fiber constant during the experiments, the fiber region where the grating was written was attached permanently to a microscope slide and small quantities of liquids with various refractive indices were dispensed with a pipette onto the grating. A second slide was used to cover the interaction region and to maintain the liquid in place by capillarity. The fiber and slides were cleaned thoroughly between experiments. The immersion liquids used in this work were water–sugar solutions providing a wide range of refractive indices from 1.38 (30% solution) to 1.49 (80%). The nominal refractive index (n_D) of all solutions was measured at a wavelength of 589.3 nm with an Abbe refractometer. We also used calibrated liquids from Cargille Corporation with refractive indices specified for all wavelengths and temperatures of interest in our measurements.¹⁷ Therefore we feel confident that our experimental conditions were sufficiently well controlled (for strain and temperature) to ensure reliable, reproducible results. The differential wavelength shifts were obtained by tracking the lowest point of the transmission spectra in select wavelength windows.

4. Results and Discussion

The first set of results pertains to the measurement of sugar water solutions. Figure 1(a) depicts an experimental grating transmission spectrum measured in air (tilt angle = 6 $^{\circ}$). For the same grating, Figs. 1(b) and 1(c) present overlapped spectra for several values of n_D ranging from 1.377 to 1.43. There is a notable shift of the high-order cladding modes while lower-order modes and the Bragg resonance are not affected. The resonance shown in Fig. 1(c) is located ~ 15 nm away from the Bragg resonance. It is clear that this cladding-mode resonance shifts by amounts that are easily measurable (with respect to the width of the resonance, ~ 100 pm FWHM). This single resonance can be used (in principle) to measure media with a range of n_D values between 1.0 and above 1.43 without ambiguity from neighboring resonances since the spacing between resonances is larger than

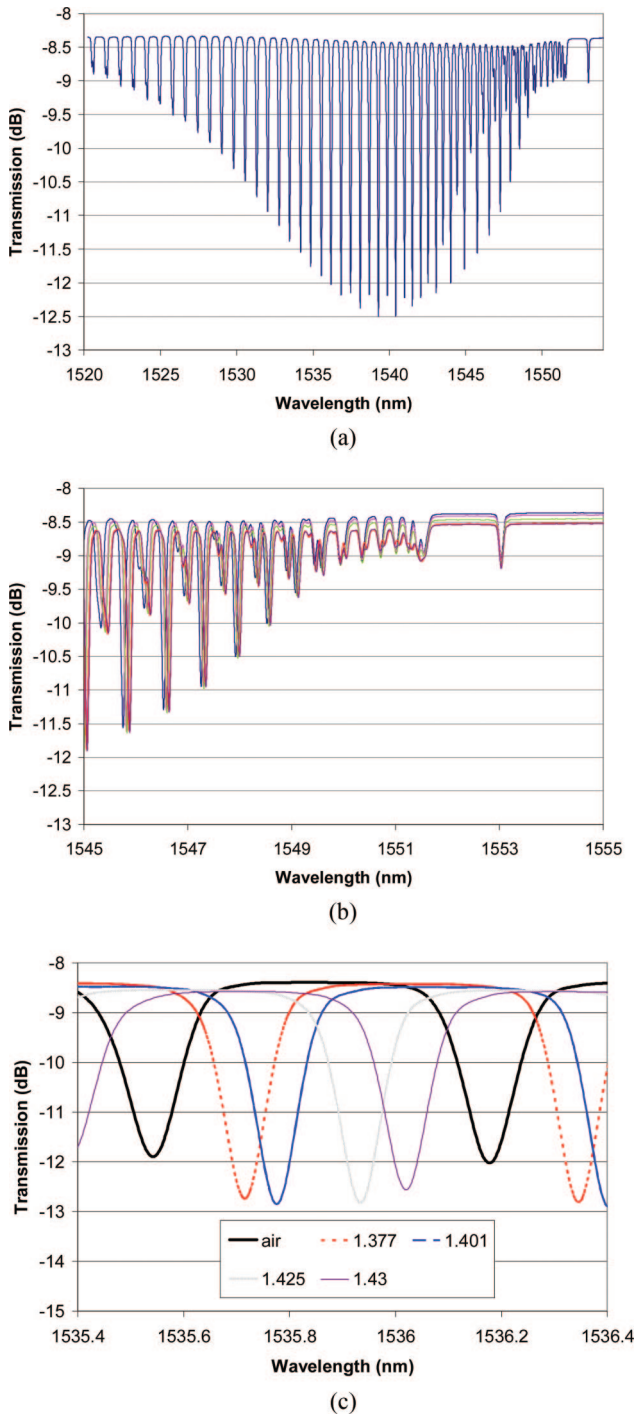


Fig. 1. (Color online) Typical experimental TFBG transmission spectra (Corning SMF-28 fiber, $\theta = 6^\circ$). (a) Full spectrum measured in air. (b) Several measurements with various refractive indices of the outer medium near the Bragg resonance. (c) Same spectra as (b) but zooming in on a particular resonance near 1535.5 nm.

600 pm while the resonance shifts by 500 pm over this range of n_D . If we now plot the relative resonance position (with respect to λ_B) as a function of n_D (Fig. 2), we see that there is a one-to-one relationship between SRI and resonance shift (another resonance, located near 17 nm away from the Bragg resonance

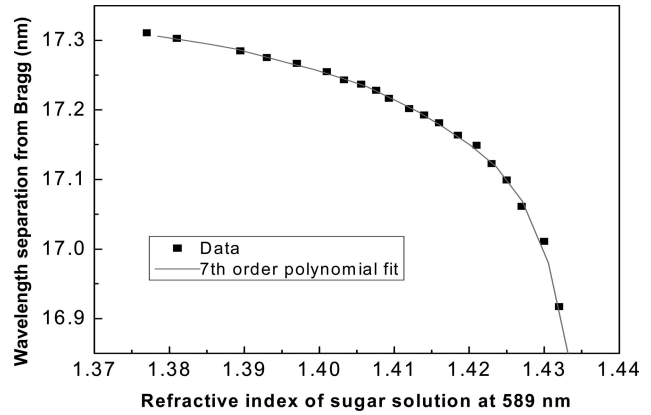


Fig. 2. Experimental shift in the distance of a cladding-mode resonance from the Bragg wavelength as a function of the refractive index of a sugar solution at 589 nm.

was used here). A seventh-order polynomial fit of the experimental results can be used as a calibration to correlate the measured wavelength shift with n_D . However, the sensitivity is quite poor for low values of SRI (20 pm/u.r.i. near $n_D = 1.38$) and increases dramatically as the SRI approaches the value at which this particular cladding mode becomes cut off (3900 pm/u.r.i. near $n_D = 1.43$). This sensitivity increase near cutoff is typical of all sensing mechanisms that rely on penetration of the evanescent field of the cladding modes into the outer medium.³ However, this is where the TFBG configuration becomes advantageous since one can select different resonances of the same sensor, depending on the refractive index range of interest, to achieve the highest sensitivity. If the refractive index range of a particular situation is not known beforehand, then a simple pattern analysis of the transmission spectrum (compared to a stored transmission spectrum in air or in pure water) will reveal immediately which modes approach cutoff and where the measuring wavelength window should be located relative to the Bragg wavelength (for maximum sensitivity). By contrast, with an LPG-based sensor only a few (and generally only one or two) cladding modes are visible in a measurement window covering several hundred nanometers. In such cases, a new sensor design (grating period or coating material) is required to optimize the sensitivity over different refractive index regions.

To demonstrate this point quantitatively, further tests were carried out with calibrated liquids in order to investigate whether we could predict the refractive index sensitivity of several mode resonances by simulations and also to determine the temperature cross sensitivity of our sensors. Figure 3 shows a comparison between predicted and measured differential wavelength shifts as a function of surrounding refractive index for various cladding-mode orders. The cladding modes are identified here by the value of $(\lambda_B - \lambda_C)$ measured when the grating is in air (i.e., the original distance of the resonance from the Bragg wavelength irrespective of the mode identity and symmetry). The predicted shifts (solid curves) were

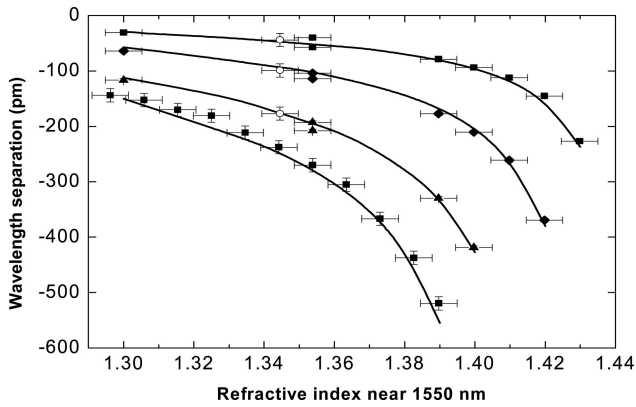


Fig. 3. Change in wavelength separation from the Bragg wavelength for four different cladding modes ($\lambda_B - 8$, -14 , -23 , and -28 nm: top to bottom) as a function of the refractive index of calibrated liquids. Solid symbols, experimental data at room temperature (23 °C); open symbols, experimental data at 50 °C; curves, simulations.

obtained with a commercially available software package¹⁷ using the refractive index profile and geometry of the standard fiber used. The fiber parameters used are core radius = 4.15 μm , cladding radius = 62.5 μm , $n(\text{core}) = 1.450699$, $n(\text{clad}) = 1.444024$, both at 1566 nm and corrected for dispersion for other wavelengths, using the dispersion of pure silica as a guide and offsetting the dispersion curves to the refractive indices given above for $\lambda = 1566$ nm. When experimental error is taken into account, all the measurements agree with values predicted from the model. For single measurements, we use an error estimate of ± 12 pm for the exact value of the wavelength distance between a resonance and the Bragg wavelength relative to its value in air, to reflect an absolute uncertainty of at least 3 pm on each wavelength measured. For some of the measurements shown in Fig. 3, five independent measurements were made with the same liquid, and the average value of the wavelength distance was calculated. In such cases, the error estimate is provided by the standard deviation of the measurements. The standard deviation for these measurements never exceeded 3 pm. The uncertainty in the value of the refractive index is given as ± 0.0002 (at 589 nm) by Cargille. For longer wavelengths, the supplier provides Cauchy coefficients to calculate the dispersion of the refractive index but with an added uncertainty of the order of 0.005. Our results seem to indicate that the actual uncertainty of the refractive index of the liquids is smaller.

To validate our claims of relative temperature independence, an additional measurement was carried out at a temperature of 50 °C (open circles in Fig. 3). When the thermo-optic coefficient of the liquid ($-3.41 \times 10^{-3}/^\circ\text{C}$) is taken into account, the refractive index values obtained from the grating also fall on the expected curve. This indicates that the sensor was able to measure the true refractive index of the liquids (within error), even though all its wavelength

resonances were shifted by ~ 265 pm due to the increase in temperature (+27 °C). The sensitivity of the SRI measurements (and simulations) reaches over 10,000 pm/u.r.i. for each of the resonances shown in Fig. 3, corresponding to better than 10^{-4} refractive index sensitivity (u.r.i./pm) between 1.38 and 1.43. The sensitivity calculated here for single resonance measurements ($10^{-4}/\text{pm}$) obviously needs to be adjusted by the wavelength measurement accuracy (~ 10 pm for the relative shift) to yield an actual sensitivity closer to 10^{-3} in SRI in our experiments. On the other hand, modern dedicated fiber grating interrogation equipment claims a wavelength measurement accuracy better than 1 pm,¹⁸ making 10^{-4} sensitivity a definite possibility. With such an instrument, we have achieved a repeatability of the measurement of the wavelength distance (standard deviation of successive measurements of a fixed experimental situation) of 0.6 pm.

If there is a need for higher sensitivity at lower values of n_{ext} , there are two design modifications that can be used to do so. First, it is possible to generate even higher-order mode resonances with the TFBG, so that accurate resonance measurements can be made further away from the Bragg resonance. This can be achieved with a larger tilt angle, as shown in Fig. 4 where cladding-mode resonances as far away as 100 nm from the Bragg wavelength are observed for tilt angles near 10° (to keep most of the spectrum within our measurement window the grating period was increased to 541 nm in this case). These resonances have effective indices near 1.25 and hence allow high sensitivity measurements in this range of values of the SRI. With the grating shown in Fig. 4, we achieved 11,200 pm/u.r.i. for a SRI near 1.31 by using the resonance at 1500 nm [see Fig. 4(b)]. The additional benefit of using resonances further away from the Bragg wavelength is that their spacing increases (to over 1200 pm in this case), thereby augmenting the range of unambiguous readings for the position of the resonance relative to its position in air (a similar effect occurs with reduced diameter cladding fibers¹⁹ but requires custom fabrication of the fibers or thinning methods, which lead to reduced mechanical strength). A second way to increase sensitivity is to use a thin high index coating on the cladding to pull out the evanescent field of cladding modes into the outside medium to enhance the overlap and sensitivity to SRI, as is commonly done for LPGs.^{20,21} It is worth repeating here that unlike devices based on LPGs, all these modes are always available with a single grating device design, and the exact wavelength of the Bragg resonance of the device is quite irrelevant (as well as the exact strength of the grating). These relaxed tolerances ensure that the mass production of such devices at very low cost is definitely possible.

Finally, the availability of several resonances within a single sensor measurement provides a way to increase the measurement accuracy by averaging the result obtained with the shifts of many cladding

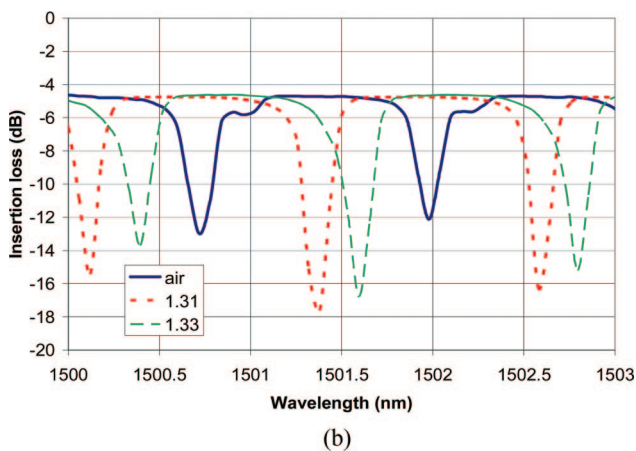
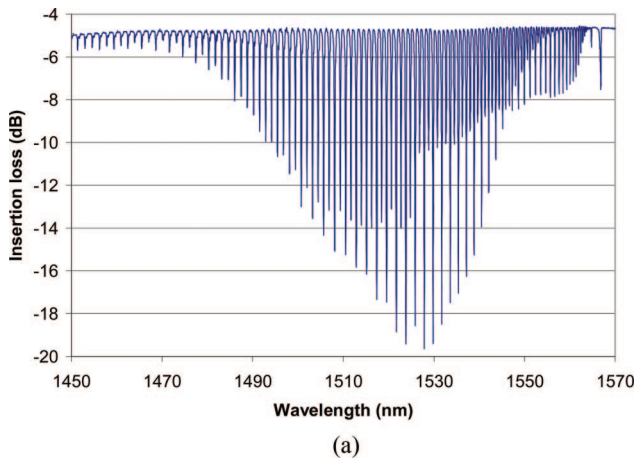


Fig. 4. (Color online) (a) Experimental transmission spectrum of a TFBG with a tilt angle of 10° ($\lambda_{\text{Bragg}} = 1566.810$ nm). (b) Shift of a resonance near 1500 nm for various external media (solid curve, SRI = 1.0; dotted curve, SRI = 1.3058; dashed curve, SRI = 1.3250; all the values are for $\lambda = 1500$ nm).

modes simultaneously. Since any systematic wavelength error is already eliminated by the fact that we are measuring relative wavelength shifts, the wavelength errors associated with each resonance should be statistically independent. Taking the results of Fig. 3 as an example, we have four independent wavelength shift measurements for each value of SRI. We can calculate a predicted SRI from the simulation for each of these measurements, take the average, and plot the results against the actual SRI as calculated from the supplier data taking into account dispersion. The result is shown in Fig. 5. In spite of the fact that the supplier only guarantees ± 0.0052 accuracy on the refractive index of the liquids for wavelengths away from 589 nm, we obtain excellent agreement between measured and expected values (as indicated by the slope of 0.999 and intercept of 5×10^{-4}) as well as very good correlation ($R^2 = 0.997$). In fact, while the refractive index predictions from single measurements have errors ranging from -0.012 to $+0.006$, the errors obtained by averaging the predictions from four resonances range only from -0.0009 to 0.001 . Even better results would be ex-

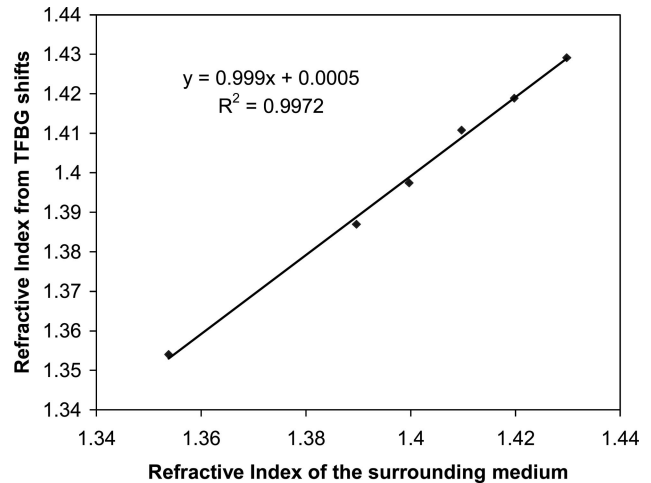


Fig. 5. Measured refractive index from the average of the predictions based on the shifts of four resonances (-8 , -14 , -23 , and -28 nm) versus actual refractive index.

pected from a more sophisticated algorithm able to average the predictions of all the available resonances.

For comparisons, refractometers based on LPGs will have sensitivities of the order of $100\text{--}1000$ nm/u.r.i. with cross sensitivity to temperature of the order of 1 nm/ $^\circ\text{C}$ and above for the absolute measurement of the wavelengths of resonances with bandwidths ranging from 10 to 100 nm.^{8,20,21} In the best cases, the sensitivity divided by the resonance bandwidth is 100 (u.r.i.)⁻¹ for LPGs, exactly equivalent to our results since it is just as easy to monitor pm shifts of 100 pm resonances as it is to monitor nanometer shifts of 100 nm resonances (easier in a way because the required spectral range of the interrogation systems is much smaller) and the same sensitivity enhancement techniques^{8,20,21} can be applied to TFBGs as to LPGs. The only differences are that TFBGs have an inherent temperature monitoring channel (the Bragg resonance), and that they provide several measurements simultaneously to either achieve the

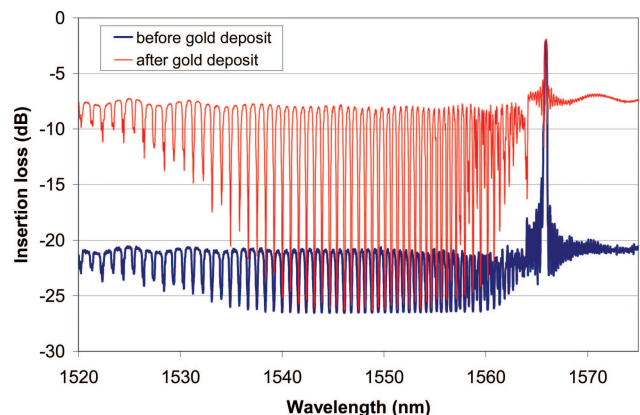


Fig. 6. (Color online) Reflection spectrum of packaged TFBG with a cleaved end downstream of the grating: bottom trace, as cleaved; top trace, with gold coating on the face of the cleave.

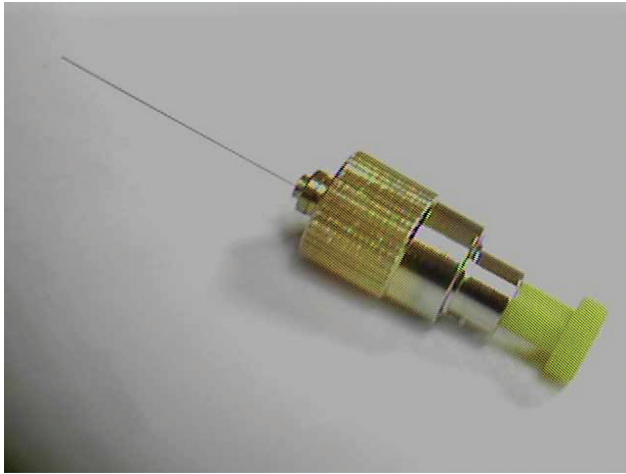


Fig. 7. (Color online) Photograph of the packaged sensor (basically a connectorized piece of fiber ~ 25 mm long with a TFBG in the length of the fiber outside the connector).

highest sensitivity over several ranges of SRI or to improve accuracy by averaging several measurements from a single sensor.

5. Practical Implementation

One final issue deals with the fact that the measurement must be made in transmission, requiring access to the sensor from both sides. For applications in small areas, it would be desirable to have a single-ended sensor located at the end of a fiber, which could then be inserted into volumes as small as a few millimeters in length by $150 \mu\text{m}$ in diameter. An easy way to achieve this is to cleave the fiber downstream from the grating section and use the broadband reflection from the fiber end to send the light back toward the source, thereby going through the grating twice and doubling the attenuation of each resonance. While a cleaved fiber offers $\sim 4\%$ of broadband reflection [Fig. 6(a)], a metallic coating can be used to increase the broadband reflectivity to near 100% [Fig. 6(b)]. For such terminated fibers, the Bragg reflection now appears as a peak in the measured power while the cladding resonances still appear as troughs. The extraction of the data poses no particular problem in this configuration (which was used for some of the data accumulated in Fig. 3). Figure 7 shows a picture of a packaged sensor: essentially a connectorized piece of fiber with the TFBG near the gold-coated far end. This configuration also ensures strain-free operation of the sensor to eliminate the effect of cross sensitivity to strain of the higher-order cladding modes.

6. Conclusion

We have shown that a TFBG can provide a measurement of refractive index with an accuracy of the order of 10^{-4} for refractive index ranges extending from 1.25 to 1.43 and independently of the temperature. The technique is based on tracking the shifts in the positions of the central wavelength of the cladding-

mode resonances and calculating their wavelength separation from the Bragg resonance. This technique exhibits advantages over other conventional techniques such as LPG sensors and etched fiber sensors while achieving similar or better sensitivity. These advantages are a single grating design for a wide range of external media refractive indices, a relative strain and temperature independence, straightforward interrogation using available equipment, the sensors require no physical modification of the fiber geometry (thus preserving the fiber mechanical strength), and much relaxed fabrication tolerances. Data extraction algorithms can improve the accuracy by taking advantage of the multiple measurements provided by a single sensor.

Finally, it must be pointed out that a scheme similar to ours but realized in multimode fiber was recently published.²² In that particular implementation, a Bragg grating is used to couple light to a multitude of backreflected core modes and cladding modes. The core mode resonances are used to monitor the ambient temperature while cladding-mode resonances acquire a differential shift due to the surrounding refractive index. We believe our method is more practical because in single-mode fibers there is no ambiguity about the temperature reference provided by the single Bragg resonance and there is no uncertainty associated with the distribution of the guided power among the multiple core modes (the transmission spectrum of a TFBG in a single-mode fiber is highly repeatable and does not depend on launch conditions in the fiber, unlike TFBGs in multimode fibers).

This work was carried out at the Carleton Laboratory for Laser Induced Photonic Structures and supported by the Natural Sciences and Engineering Research Council of Canada, the Canada Foundation for Innovation, the Center for Photonic Fabrication Research, and LxSix Photonics. The loan of a Fiber Grating interrogator by Micron Optics, Incorporated is gratefully acknowledged.

References

1. T. M. Niemczyk, "Refractive index measurement," in *Physical Methods in Modern Chemical Analysis*, T. Kuwana, ed. (Academic, 1980), Vol. 2, pp. 337–400.
2. V. Bathia, "Applications of long-period gratings to single and multi-parameter sensing," *Opt. Express* **4**, 457–466 (1999).
3. S. W. James and R. P. Tatam, "Optical fiber long-period grating sensors: characteristics and application," *Meas. Sci. Technol.* **14**, R49–R61 (2003).
4. N. D. Rees, S. W. James, R. P. Tatam, and G. J. Ashwell, "Optical fiber long-period gratings with Langmuir–Blodgett thin-film overlays," *Opt. Lett.* **27**, 686–688 (2002).
5. A. N. Chryssis, S. M. Lee, S. B. Lee, S. S. Saini, and M. Dagenais, "High sensitivity evanescent field fiber Bragg grating sensor," *IEEE Photon. Technol. Lett.* **17**, 1253–1255 (2005).
6. A. Iadicco, S. Campopiano, A. Cutolo, M. Giordano, and A. Cusano, "Nonuniform thinned fiber Bragg gratings for simultaneous refractive index and temperature measurements," *IEEE Photon. Technol. Lett.* **17**, 1495–1497 (2005).
7. H. J. Patrick, "Analysis of the response of long period fiber gratings to external index of refraction," *J. Lightwave Technol.* **16**, 1606–1612 (1998).

8. T. Allsop, F. Floreani, K. P. Jedrzejewski, P. V. S. Marques, R. Romero, D. J. Webb, and I. Bennion, "Spectral characteristics of tapered LPG device as a sensing element for refractive index and temperature," *J. Lightwave Technol.* **24**, 870–878 (2006).
9. G. Laffont and P. Ferdinand, "Tilted short-period fibre-Bragg-grating induced coupling to cladding modes for accurate refractometry," *Meas. Sci. Technol.* **12**, 765–770 (2001).
10. C. Caucheteur and P. Megret, "Demodulation technique for weakly tilted fiber Bragg grating refractometer," *IEEE Photon. Technol. Lett.* **17**, 2703–2705 (2005).
11. C. Chen, L. Xiong, A. Jafari, and J. Albert, "Differential sensitivity characteristics of tilted fiber Bragg grating sensors," in *Fiber Optic Sensor Technology and Applications IV*, M. A. Marcus, B. Culshaw, and J. P. Dakin, eds., *Proc. SPIE* **6004**, 600413 (2005).
12. T. Erdogan, "Cladding-mode resonances in short- and long period fiber grating filters," *J. Opt. Soc. Am. A* **14**, 1760–1773 (1997).
13. Technical specifications for fused silica (Technical products division, Advanced Products Department, Corning Inc. MP-21-4, Corning, N.Y. 14831).
14. C. Chen and J. Albert, "Strain-optic coefficients of the individual cladding modes of a single mode fiber: theory and experiment," *Electron. Lett.* **43**, 21–22 (2006).
15. K. O. Hill, B. Malo, F. Bilodeau, D. C. Johnson, and J. Albert, "Bragg gratings fabricated in monomode photosensitive optical fiber by UV exposure through a phase mask," *Appl. Phys. Lett.* **62**, 1035–1037 (1993).
16. P. J. Lemaire, R. M. Atkins, V. Mizrahi, and W. A. Reed, "High pressure H₂ loading as a technique for achieving ultrahigh UV photosensitivity and thermal sensitivity in GeO₂ doped optical fibres," *Electron. Lett.* **29**, 1191–1193 (1993).
17. Optigrating, from the Optiwave Corporation (Ottawa, Canada).
18. High resolution swept laser interrogator, Model Si720, from Micron Optics, Inc., Atlanta, Ga.
19. C. Chen, C. Caucheteur, P. Megret, and J. Albert, "Sensitivity of tilted fiber Bragg grating sensors with different cladding thicknesses," in *18th Conference on Optical Fiber Sensors (OFS-18)*, (2006), paper TuE31.
20. A. Cusano, A. Iadicicco, P. Pilla, L. Contessa, S. Campopiano, and A. Cutolo, "Cladding mode reorganization in high-refractive index-coated long-period gratings: effects on the refractive-index sensitivity," *Opt. Lett.* **30**, 2536–2538 (2005).
21. J. Yang, L. Yang, C. Xu, C. Xu, W. Huang, and Y. Li, "Long-period grating refractive index sensor with a modified cladding structure for large operational range and high sensitivity," *Appl. Opt.* **45**, 6142–6147 (2006).
22. C. Zhao, X. Yang, M. S. Demokan, and W. Jin, "Simultaneous temperature and refractive index measurements using a 3° slanted multimode fiber Bragg grating," *J. Lightwave Technol.* **24**, 879–883 (2006).